Tetrahedral vs Octahedral Zinc Complexes with Ligands of Biological Interest: A DFT/CDM Study

Todor Dudev[†,§] and Carmay Lim*[,†,‡]

Contribution from the Institute of Biomedical Sciences, Academia Sinica, Taipei 11529, Taiwan, R.O.C., and Department of Chemistry, National Tsing Hua University, Hsinchu 300, Taiwan, R.O.C.

Received March 22, 2000. Revised Manuscript Received August 25, 2000

Abstract: To elucidate the most preferable, ground-state coordination geometry for zinc complexes in a protein environment, the free energies of isomerization between hexa- and tetracoordinated structures containing Zn^{2+} bound to water and ligands of biological interest were evaluated. Density functional theory using the 6-31++G-(2d,2p) basis set was employed in calculating isomerization free energies in the gas phase, while continuum dielectric theory was used to compute solvation free energies of the zinc clusters in different dielectric media. The results show that the lowest-energy ground-state coordination number of zinc bound to one acidic or two or more neutral protein ligands is 4. The observed decrease in the coordination number of zinc upon protein binding reflects primarily the requirements of the metal and ligands, rather than the constraints of the protein matrix on the metal. Our finding that the *tetrahedral* zinc complexes in protein cavities generally represent the optimal, least strained structures among various zinc polyhedra may explain why four-coordinate zinc is chosen to play a structural role in zinc fingers and enzymes.

Introduction

Zinc can play a structural and/or catalytic role in proteins. The most well studied proteins in which zinc serves a structural role belong to the zinc-finger family, which is involved in nucleic acid binding and gene regulation.[1] In zinc-finger proteins, zinc is tetrahedrally coordinated to histidines and/or cysteines, which form three distinct types of metal-binding motifs: His-His-Cys-Cys, His-Cys-Cys-Cys, or Cys-Cys-Cys-Cys.[2−4] In addition to its structural role, zinc plays an essential role in many enzymes involved in virtually all aspects of metabolism. Currently, there are about 300 known zinc enzymes. The most commonly found ligand in zinc catalytic binding sites is histidine, but cysteine, aspartic acid, and glutamic acid residues are also seen coordinated to the metal.[5] As a rule, the enzyme donates three ligands, leaving the fourth position for a (catalytic) water.

Zinc is flexible with respect to the number of ligands it can adopt in its first coordination shell. Although in aqueous solution Zn^{2+} is coordinated to six water molecules,[6] in both zinc-finger proteins and enzymes, zinc is usually *tetrahedrally* coordinated, but in some catalytic binding sites it is found pentacoordinated and, rarely, hexacoordinated.[7] In sharp contrast, Mg^{2+}, which is also divalent with an ionic radius (0.65 Å) similar to that of Zn^{2+} (0.74 Å), is usually octahedrally coordinated both in aqueous solution and in proteins.[8] It is not clear if the observed decrease in the coordination number of zinc upon protein binding reflects the constraints of the protein matrix on zinc[9] or the specific physicochemical requirements of the metal and/or ligands. In other words, the lowest-energy, ground-state coordination geometry for zinc complexes in proteins has not been unambiguously established. These questions are of prime importance in elucidating the mechanism(s) of zinc binding to proteins as well as the catalytic role of zinc.

Most theoretical studies have been dedicated to evaluating the thermodynamical parameters of the Zn^{2+} *hydration* process.[8,10−15] The binding energies and, in some cases, the binding free energies of the stepwise water binding to Zn^{2+},

$$[Zn(H_2O)_n]^{2+} + H_2O \rightarrow [Zn(H_2O)_{n+1}]^{2+} \quad (n = 0-5) \quad (1)$$

have been calculated by employing different levels of ab initio calculations. In addition to the all-inner-sphere complexes $[Zn(H_2O)_n]^{2+}$ ($n = 1-6$), a variety of mixed inner- and outer-sphere clusters $\{[Zn(H_2O)_n]\cdot(H_2O)_m\}^{2+}$ ($n = 3-6$; $m = 1-12$) have been studied, and their total binding energies have been compared to those of the respective all-inner-sphere complexes

[†] Academia Sinica.
[‡] National Tsing Hua University.
[§] On leave from the Department of Chemistry, University of Sofia, Bulgaria.

(1) Berg, J. M.; Godwin, H. A. *Annu. Rev. Biophys. Biomol. Struct.* **1997**, *26*, 357.
(2) Miller, J.; McLachlan, A. D.; Klug, A. *EMBO J.* **1985**, *4*, 1609.
(3) Summers, M. F.; South, T. L.; Kim, B.; Hare, D. *Biochemistry* **1990**, *29*, 329.
(4) Petkovich, M.; Brand, N. J.; Krust, A.; Chambon, P. *Nature* **1987**, *330*, 444.
(5) Jernigan, R.; Raghunathan, G.; Bahar, I. *Curr. Opin. Struct. Biol.* **1994**, *4*, 256.
(6) Marcus, Y. *Chem. Rev.* **1988**, *88*, 1475.
(7) Alberts, I. L.; Nadassy, K.; Wodak, S. J. *Protein Sci.* **1998**, *7*, 1700.
(8) Bock, C. W.; Katz, A. K.; Markham, G. D.; Glusker, J. P. *J. Am. Chem. Soc.* **1999**, *121*, 7360.
(9) Williams, R. J. P. *Eur. J. Biochem.* **1995**, *234*, 363.
(10) Stromberg, D.; Sandstrem, M.; Wahlgren, U. *Chem. Phys. Lett.* **1990**, *172*, 49.
(11) Bock, C. W.; Katz, A. K.; Glusker, J. P. *J. Am. Chem. Soc.* **1995**, *117*, 3754.
(12) Lee, S.; Kim, J.; Park, J. K.; Kim, K. S. *J. Phys. Chem.* **1996**, *100*, 14329.
(13) Katz, A. K.; Glusker, J. P.; Beebe, S. A.; Bock, C. W. *J. Am. Chem. Soc.* **1996**, *118*, 5752.
(14) Hartmann, M.; Clark, T.; van Eldik, R. *J. Am. Chem. Soc.* **1997**, *119*, 7843.
(15) Pavlov, M.; Siegbahn, P. E. M.; Sandström, M. *J. Phys. Chem. A* **1998**, *102*, 219.

10.1021/ja0010296 CCC: $19.00
Published on Web 11/01/2000

containing the same number of water molecules. (The notation, $\{[M(H_2O)_p(L)_q]\cdot(H_2O)_m\}^{2+}$, where $p + q = n$, denotes a divalent metal ion, M^{2+}, bound to n ligands (p waters and q nonaqua ligands) in the first coordination shell, and m water molecules in the second hydration layer; for brevity, it is referred to as an $(n + m)$ complex).

All the theoretical studies have shown that zinc, unlike magnesium for example, does not have a strong preference for a particular number of water molecules in its first coordination layer and can accommodate four, five, or six water ligands; the calculated *energy* differences between isomeric $[Zn(H_2O)_6]^{2+}$, $\{[Zn(H_2O)_5]\cdot(H_2O)_1\}^{2+}$, and $\{[Zn(H_2O)_4]\cdot(H_2O)_2\}^{2+}$ complexes differ by only a few kilocalories per mole. However, there is no consensus regarding the most stable structure among the three isomers. The MP2(FC)/HUZSP*//RHF/HUZSP* calculations by Bock et al.[11] and the B3LYP/6-311+G(2d,2p)//B3LYP/LANL-2DZ calculations by Pavlov et al.[15] predict the tetrahedral (4 + 2) complex to be the most stable structure as it is *lower* in *energy* (by 0.1 and 3.4 kcal/mol, respectively) than its octahedral $[Zn(H_2O)_6]^{2+}$ counterpart. However, more recent MP2(FULL)/6-311++G**//HF/HUZ* calculations by Bock et al.[8] and MP2/TZ2P//HF/TZ2P calculations by Lee et al.[12] predict the tetrahedral (4 + 2) complex to be *higher* in *energy* (by 1.4 and 3.1 kcal/mol, respectively) than the octahedral structure. Note that diffuse functions, which have been shown to be important in computing the binding enthalpies and free energies of metals,[15,16] are not included in the HUZSP*, HUZ*, and TZ2P basis sets. Pavlov et al.[15] also examined bigger clusters with a more complete second coordination layer and found that the tetrahedral $\{[Zn(H_2O)_4]\cdot(H_2O)_8\}^{2+}$ complex is more stable (by 5.6 kcal/mol) than the octahedral $\{[Zn(H_2O)_6]\cdot(H_2O)_6\}^{2+}$ cluster. All these studies report gas-phase energies and/or enthalpies rather than *solution free* energies, and, therefore, the effect of the dielectric media (protein or aqueous solution) on the energy of binding has not been considered.

Theoretical studies dedicated to assessing the role of nonaqua ligands on the geometry of zinc complexes are scarce, and, so far, no systematic efforts have been made to solve this problem. In a specific study on alcohol dehydrogenase, Ryde[17] employed ab initio MP2/DZ//HF/DZ calculations to model the active site (consisting of two cysteines, one histidine, and one water bound to a zinc cation) and some reaction intermediates possessing different coordination geometries. The cysteinate ligand was modeled as HS^- and the histidine side chain as ammonia or, in some cases, imidazole. Tetra-, penta-, and hexacoordinated $Zn(HS)_2X(H_2O)_{0-2}L$ (where X = ammonia or imidazole, and L = catalytic water, methanol, ethanol, or the corresponding anions or aldehydes) structures were examined, and their relative stabilities were assessed. In the gas phase the *tetracoordinated* species (with one or two water molecules in the outer coordination shell) was found to be more stable than the respective penta- and hexacoordinated inner-sphere complexes by about 4 and 10 kcal/mol, respectively. In a subsequent publication, by employing combined QM/MM calculations for the same enzyme, Ryde showed that in the protein environment the energy difference between isomeric *tetra-* and *pentacoordinated* zinc complexes widens in favor of the former and ranges between 24 and 48 kcal/mol.[17,18]

The primary goal of this paper is to elucidate the most preferable, ground-state coordination geometry for zinc complexes in a protein environment. To this end, the free energies of isomerization between hexa- and tetracoordinated structures containing Zn^{2+} bound to water and ligands of biological interest were evaluated. The nonaqua ligands are simple organic molecules that model the amino acid residues most commonly found coordinated to zinc in proteins (see above). These are (1) imidazole (for the neutral histidine side chain), (2) methanethiolate (for ionized cysteine), and (3) formate (for deprotonated aspartic and glutamic acids). Density functional theory (DFT) using the 6-31++G(2d,2p) basis set was employed in computing isomerization free energies in the gas phase, and continuum dielectric theory was used to estimate solvation free energies of the zinc clusters in different dielectric media (see Methods). The stabilities of isomeric hexa- and tetracoordinated zinc complexes in the gas phase and various dielectric media were assessed, and the results are contrasted with those for some Mg^{2+} clusters (see Results). The factors governing the geometry of the first coordination shell in metal clusters were identified. The implications of the cluster geometry on the process of zinc binding to proteins and enzyme activation are presented (see Discussion).

Methods

DFT Calculations. These employed Becke's three-parameter hybrid method[19] in conjunction with the Lee, Yang, and Parr correlation functional.[20] Initially, to determine the optimal basis set for the zinc complexes, increasing basis sets, 6-31+G*, 6-31++G**, 6-311++G**, 6-31++G(2d,2p), 6-311++G(2d,2p), and 6-31++G(2df,2p), were used to compute the free energies of water → chloride substitution reactions, for which experimental results were available for calibration (see Results). Subsequently, the 6-31++G(2d,2p) basis set, which was found to be a reasonable compromise between performance and computational costs from the calibration study (see Results), was employed for the rest of the calculations. This basis set has two sets of polarization functions as well as diffuse functions on all atoms.

Full geometry optimization for the entire series of complexes was carried out at the B3LYP/6-31++G(2d,2p) level using the Gaussian 98 program.[21] Vibrational frequencies were then computed at the same level of theory to verify that each cluster was at the minimum of its potential energy surface. No imaginary frequency was found in any of the clusters. After the frequencies were scaled by an empirical factor of 0.9613,[22] the zero-point energy (ZPE), thermal energy (E_T), and entropy (S) corrections were evaluated using standard statistical mechanical formulas.[23] The differences in ΔE_{elec}, ΔZPE, ΔE_T, and ΔS between the products and reactants were employed to compute the free energy of isomerization between hexa- and tetracoordinated complexes at room temperature, T = 298.15 K, according to the following expression:

$$\Delta G^1 = \Delta E_{elec} + \Delta ZPE + \Delta E_T - T\Delta S \qquad (2)$$

Equation 2 was also used to compute the free energy for $M^{2+} + nH_2O \rightarrow [M(H_2O)_n]^{2+}$, where $M = Zn^{2+}$ or Mg^{2+} and $n = 1-6$. These

(16) Markham, G. D.; Glusker, J. P.; Bock, C. L.; Trachtman, M.; Bock, C. W. *J. Am. Chem. Soc.* **1996**, *100*, 3488.
(17) Ryde, U. *Int. J. Quantum Chem.* **1994**, *52*, 1229.
(18) Ryde, U. *Proteins: Struct., Funct. Genet.* **1995**, *21*, 40; *J. Comput.-Aided Mol. Des.* **1996**, *10*, 153.
(19) Becke, A. D. *J. Chem. Phys.* **1993**, *98*, 5648.
(20) Lee, C.; Yang, W.; Parr, R. G. *Phys. Rev.* **1988**, *B37*, 785.
(21) Frisch, M. J.; Trucks, G. W.; Schlegel, H. B.; Scuseria, G. E.; Robb, M. A.; Cheeseman, J. R.; Zakrzewski, V. G.; Montgomery, J. A., Jr.; Stratmann, R. E.; Burant, J. C.; Dapprich, S.; Millam, J. M.; Daniels, A. D.; Kudin, M. C.; Strain, K. N.; Farkas, O.; Tomasi, J.; Barone, V.; Cossi, M.; Cammi, R.; Mennucci, B.; Pomelli, C.; Adamo, C.; Clifford, S.; Ochterski, J.; Petersson, G. A.; Ayala, P. Y.; Cui, Q.; Morokuma, K.; Malick, D. K.; Rabuck, A. D.; Raghavachari, K.; Foresman, J. B.; Cioslowski, J.; Ortiz, J. V.; Stefanov, B. B.; Liu, G.; Liashenko, A.; Piskorz, P.; Komaromi, I.; Gomperts, R.; Martin, R. L.; Fox, D. J.; Keith, T.; Al-Laham, M. A.; Peng, C. Y.; Nanayakkara, A.; Gonzalez, C.; Challacombe, M.; Gill, P. M. W.; Johnson, B.; Chen, W.; Wong, M. W.; Andres, J. L.; Gonzalez, C.; Head-Gordon, M.; Replogle, E. S.; Pople, J. A. *Gaussian 98*, Revision A.5; Gaussian, Inc.: Pittsburgh, 1998.
(22) Wong, M. W. *Chem. Phys. Lett.* **1996**, *256*, 391.
(23) McQuarrie, D. A. *Statistical Mechanics*; Harper and Row: New York, 1976.

energies were not corrected for basis set superposition error since previous works have shown that the dominant effect of the basis set superposition error is not on the total energy,[15] but on properties such as the dipole moment and the polarizability, and BSSE corrections did not improve the accuracy of the results.[24,25]

Continuum Dielectric Calculations. The reaction free energy in a given environment characterized by a dielectric constant $\epsilon = x$ can be calculated according to the following thermodynamic cycle:

$$\begin{array}{ccc} \text{reactants } (\epsilon = 1) & \xrightarrow{\Delta G^1} & \text{products } (\epsilon = 1) \\ \Delta G_{\text{solv}}{}^x(\text{reactants}) \downarrow & & \downarrow \Delta G_{\text{solv}}{}^x(\text{products}) \\ \text{reactants } (\epsilon = x) & \xrightarrow[\Delta G^x]{} & \text{products } (\epsilon = x) \end{array} \quad (3)$$

ΔG^1 is the gas-phase free energy computed using eq 2. $\Delta G_{\text{solv}}{}^x$ is the free energy for transferring a molecule in the gas phase to a solvent medium characterized by a dielectric constant x. By solving Poisson's equation using finite difference methods[26,27] to yield $\Delta G_{\text{solv}}{}^x$ (see below), the reaction free energy in an environment modeled by dielectric constant x, ΔG^x, can be computed from

$$\Delta G^x = \Delta G^1 + \Delta G_{\text{solv}}{}^x(\text{products}) - \Delta G_{\text{solv}}{}^x(\text{reactants}) \quad (4)$$

The continuum dielectric calculations employed a $71 \times 71 \times 71$ lattice centered on the metal cation with a grid spacing of 0.25 Å, ab initio geometries, and natural bond orbital (NBO) atomic charges.[28] The low-dielectric region of the solute was defined as the region inaccessible to contact by a 1.4-Å sphere rolling over the molecular surface. This region was assigned a dielectric constant of 2 to account for the electronic polarizability of the solute. The molecular surface was defined by effective solute radii, which were obtained by adjusting the CHARMM (version 22)[29] van der Waals radii to reproduce the experimental hydration free energies of the metal cations and ligands as well as the solution free energies of water → chloride substitution reactions. The radii employed in the study are (in Å) $R_{\text{Zn}} = 1.4$, $R_{\text{Mg}} = 1.5$, $R_{\text{Cl}} = 2.2$, $R_{\text{O}}(\text{H}_2\text{O}) = 1.69$, $R_{\text{O}}(\text{HCOO}^-) = 1.65$, $R_{\text{H}}(\text{H}_2\text{O}) = 1.0$, $R_{\text{H}}(\text{C,N}) = 1.468$, $R_{\text{C}} = 1.9$, $R_{\text{N}} = 1.7$. (Note that these radii have been parametrized for B3LYP/6-31++G(2d,2p) geometries and NBO charges.) At the calibration stage, experimental hydration free energies of water (−6.3 kcal/mol) and Cl^- (−77 kcal/mol) were used to compute the solution free energies of water → chloride substitution reactions (see Results).

The dielectric constant of a protein is generally assumed to range between 2 and 4.[26,30] Thus, Poisson's equation was solved with an external dielectric constant equal to 2 or 4 to simulate buried or partially buried binding sites, and 80 to characterize fully solvent-exposed binding sites. The difference between the computed electrostatic potential in a given dielectric medium ($\epsilon = x$) and in the gas phase ($\epsilon = 1$) yielded the solvation free energy $\Delta G_{\text{solv}}{}^x$ of the metal complex.

Results

Calibration of the DFT and Continuum Dielectric Calculations. The series of zinc chloride complexes, $[\text{Zn}(\text{H}_2\text{O})_m\text{Cl}_p]^{2-p}$ ($m = 2-5$; $p = 1-4$), was chosen for calibration purposes because (i) the experimental solution free energies of stepwise water → chloride substitution are available,[31,32] and (ii) the zinc clusters are small enough to allow calculations with very large basis sets. Since the hydrated zinc cation is known to be octahedrally coordinated[6] in aqueous solution, all six water molecules in $[\text{Zn}(\text{H}_2\text{O})_6]^{2+}$ were placed in the first coordination layer of the cation. In contrast, the dichloride and tetrachloride zinc complexes are known to be *tetrahedrally* coordinated with the Cl^- ligand in the inner coordination shell.[6,11] This observation is also supported by our ab initio calculations, which show that the gas-phase free energies, $\Delta G_{\text{subst}}{}^1$, for the first two water → chloride substitution reactions are more favorable for *tetrahedral* products (with two water molecules in the second coordination sphere) than for the respective octahedral clusters. The zinc monochloride and dichloride *tetrahedral* complexes were calculated to be more stable than the respective *octahedral* complexes by −4.5 and −8.6 kcal/mol, respectively, at the B3LYP/6-31++G(2d,2p) level. Furthermore, stationary points for zinc octahedral complexes containing three or four Cl^- could not be found since they isomerized into tetrahedral (4 + 2) complexes during optimization. Based on these findings, only *tetrahedral* (4 + 2) chloride products were considered.

The following substitution reactions were modeled:

$$[\text{Zn}(\text{H}_2\text{O})_6]^{2+} + \text{Cl}^- \rightarrow \{[\text{Zn}(\text{H}_2\text{O})_3\text{Cl}]\cdot(\text{H}_2\text{O})_2\}^+ + \text{H}_2\text{O} \quad (5)$$

$$\{[\text{Zn}(\text{H}_2\text{O})_3\text{Cl}]\cdot(\text{H}_2\text{O})_2\}^+ + \text{Cl}^- \rightarrow \{[\text{Zn}(\text{H}_2\text{O})_2\text{Cl}_2]\cdot(\text{H}_2\text{O})_2\}^0 + \text{H}_2\text{O} \quad (6)$$

$$\{[\text{Zn}(\text{H}_2\text{O})_2\text{Cl}_2]\cdot(\text{H}_2\text{O})_2\}^0 + \text{Cl}^- \rightarrow \{[\text{Zn}(\text{H}_2\text{O})\text{Cl}_3]\cdot(\text{H}_2\text{O})_2\}^- + \text{H}_2\text{O} \quad (7)$$

$$\{[\text{Zn}(\text{H}_2\text{O})\text{Cl}_3]\cdot(\text{H}_2\text{O})_2\}^- + \text{Cl}^- \rightarrow \{[\text{ZnCl}_4]\cdot(\text{H}_2\text{O})_2\}^{2-} + \text{H}_2\text{O} \quad (8)$$

The gas-phase free energies of the water → chloride exchange reactions (eqs 5−8), evaluated at the B3LYP level of theory with different basis sets, are presented in Table 1. The different basis sets produce similar results, with $\Delta G_{\text{subst}}{}^1$ varying by less than 4.5 kcal/mol. As the basis set increases in size, $\Delta G_{\text{subst}}{}^1$ becomes more negative (or less positive) and appears to converge from the 6-31++G(2d,2p) basis set onward. For the last three basis sets in Table 1, the $\Delta G_{\text{subst}}{}^1$ numbers change by ≤1 kcal/mol; hence, the 6-31++G(2d,2p) basis set, being the least expensive among the higher basis sets, was chosen for subsequent calculations.

Hydration free energies for the zinc clusters were computed using the B3LYP/6-31++G(2d,2p) optimized structures and NBO charges. These $\Delta G_{\text{solv}}{}^{80}$ values together with B3LYP/6-31++G(2d,2p) $\Delta G_{\text{subst}}{}^1$ numbers from Table 1 and experimental hydration free energies of water (−6.3 kcal/mol) and Cl^- (−77 kcal/mol) were used to compute the solution free energies for eqs 5−8, which are compared with the respective experimental values[31,32] in Table 2. Although the experimental $\Delta G_{\text{subst}}{}^{80}$ error bars were not reported, the $\Delta G_{\text{subst}}{}^{80}$ numbers from different sources for reactions 5 and 6 seem to indicate that the accuracy of the experimental data is probably in the range of ±1 kcal/mol. Since the calculated free energies deviate from the experimental observables by less than 1 kcal/mol, the agreement appears to be acceptable.

Relative Stability of Octahedral vs Tetrahedral Zinc Complexes. Two types of zinc complexes were examined: octahedral $[\text{Zn}(\text{H}_2\text{O})_n\text{L}_{6-n}]^{2+}$ ($n = 4-6$) complexes with six aqua and nonaqua ligands in the first coordination shell, and

(24) Dudev, T.; Cowan, J. A.; Lim, C. *J. Am. Chem. Soc.* **1999**, *121*, 7665.
(25) Glendening, E. D.; Feller, D. *J. Phys. Chem.* **1996**, *100*, 4790.
(26) Gilson, M. K.; Honig, B. *Biopolymers* **1986**, *25*, 2097.
(27) Lim, C.; Bashford, D.; Karplus, M. *J. Phys. Chem.* **1991**, *95*, 5610.
(28) Reed, A. E.; Curtiss, L. A.; Weinhold, F. *Chem. Rev.* **1988**, *88*, 899.
(29) Brooks, B. R.; Bruccoleri, R. E.; Olafson, B. D.; States, D. J.; Swaminathan, S.; Karplus, M. *J. Comput. Chem.* **1983**, *4*, 187.
(30) Harvey, S. C.; Hoekstra, P. *J. Phys. Chem.* **1972**, *76*, 2987.
(31) *Handbook of Analytical Chemistry*; McGraw-Hill: New York, 1963.
(32) Dean, J. A. *Lange's Handbook of Chemistry*, 13th ed.; McGraw-Hill: New York, 1987.

Table 1. Gas-Phase Free Energies, ΔG_{subst}^{1}, for $\{[Zn(H_2O)_mCl_p]\cdot(H_2O)_n\}^{2-p} + Cl^- \rightarrow \{[Zn(H_2O)_{m+n-3}Cl_{p+1}]\cdot(H_2O)_2\}^{1-p} + H_2O$ (Eqs 5−8)[a]

reaction, $(m+n)$, p	ΔG_{subst}^{1} (kcal/mol)					
	6-31+G*	6-31++G**	6-311++G**	6-31++G (2d,2p)	6-311++G (2d,2p)	6-31++G (2df,2p)
(6 + 0), 0	−201.4	−202.6	−203.5	−204.8	−205.3	−205.8
(3 + 2), 1	−121.6	−122.2	−122.3	−125.4	−125.7	−125.3
(2 + 2), 2	−37.5	−38.0	−39.2	−40.2	−40.7	−40.5
(1 + 2), 3	35.3	35.0	34.4	34.4	34.7	34.5

[a] ΔG_{subst}^{1} values were computed from eq 2 using fully optimized structures at the B3LYP level.

Table 2. Calculated and Experimental Solution Free Energies, ΔG_{subst}^{80}, for $\{[Zn(H_2O)_mCl_p]\cdot(H_2O)_n\}^{2-p} + Cl^- \rightarrow \{[Zn(H_2O)_{m+n-3}Cl_{p+1}]\cdot(H_2O)_2\}^{1-p} + H_2O$

reaction, $(m+n)$, p	ΔG_{subst}^{80} (kcal/mol)	
	calcd[a]	exptl
(6 + 0), 0	−0.3	−0.6[b], 0.3[c]
(3 + 2), 1	0.8	−0.2[b], 0.5[c]
(2 + 2), 2	0.9	0.1[a]
(1 + 2), 3	0.4	0.4[a]

[a] ΔG_{subst}^{80} values were computed from eq 4 using B3LYP/6-31++G (2d,2p) ΔG_{subst}^{1} from Table 1, experimental hydration free energies of water (−6.3 kcal/mol) and Cl^- (−77 kcal/mol), and computed hydration free energies of the zinc clusters. [b] From ref 32. [c] From ref 31.

tetrahedral $\{[Zn(H_2O)_nL_{4-n}]\cdot(H_2O)_2\}^{2+}$ ($n = 2-4$) complexes with four ligands in the first coordination shell and two water molecules in the second coordination shell. The structures of the octahedral and tetrahedral zinc complexes optimized at the B3LYP/6-31++G(2d,2p) level are illustrated in Figures 1−4, while the computed free energies of isomerization between the two types of clusters for various dielectric media are listed in Table 3. The results for the zinc clusters are compared with the corresponding free energy of isomerization between octahedral and tetrahedral Mg^{2+} complexes in some cases.

(i) Complexes with Water. The $[Zn(H_2O)_6]^{2+}$ and $\{[Zn(H_2O)_4]\cdot(H_2O)_2\}^{2+}$ structures are shown in Figure 1. The (4 + 2)-hydrated Zn^{2+} complex (Figure 1B) is the preferred structure in the gas phase, being more stable by −3.7 kcal/mol than the octahedral cluster (Table 3). However, the octahedral complex is better solvated than the tetrahedral cluster, and, consequently, it becomes the dominant species in aqueous solution. The 6 → (4 + 2) isomerization free energy is positive even in a low dielectric medium ($\epsilon \geq 2$). Unlike zinc, Mg^{2+} shows a strong preference for an octahedral arrangement of water ligands in its first shell both in the gas phase and in aqueous solution: the 6 → (4 + 2) isomerization free energy is positive for ϵ ranging from 1 to 80 (Table 3). Note that for both metals, solvation effects favor the six-coordinate octahedral structure rather than its four-coordinate tetrahedral counterpart, so that the former is dominant in aqueous solution.

(ii) Complexes with One Heavy Ligand. The fully optimized structures of octahedral and tetrahedral zinc complexes containing five water molecules and one heavy ligand (imidazole or formate or methylthiolate) are illustrated in Figures 2 and 3. With a heavy ligand in the first coordination shell, the gas-phase free energy difference between octahedral and tetrahedral zinc complexes, which is −3.7 kcal/mol for the zinc hydrates, increases further: ΔG_{isom}^{1} for the monosubstituted clusters varies between −8.4 and −9.6 kcal/mol (see Table 3). The favorable ΔG_{isom}^{1} is due mainly to the enthalpic term, but for the complexes with one negatively charged formate, the entropic contribution, which is positive, is also significant. In the case of zinc bound to five water molecules and a methylthiolate, a stationary point for an octahedral complex could not be located: optimization of various octahedral initial structures resulted in a spontaneous conversion to a 4 + 2 tetrahedral geometry (Figure 3). In a protein, zinc prefers to be tetrahedrally bound to an imidazole if the metal-binding site is buried but octahedrally coordinated if the site is accessible to solvent ($\epsilon > 4$). In contrast, zinc is predicted to be tetrahedrally coordinated to one formate in either buried or solvent-exposed sites.

As in the case of magnesium hydrates, the 6 → (4 + 2) isomerization free energy for Mg^{2+} complexes containing one heavy ligand (formate or imidazole) is positive in both the gas phase and the condensed phase, indicating a strong preference for magnesium to adopt an octahedral geometry. However, due to the small magnitude of the gas-phase isomerization free energy (1.7 kcal/mol) for Mg^{2+} complexed to an imidazole, a tetrahedral structure should not be ruled out in the gas phase.

(iii) Complexes with Two Heavy Ligands. Complexes of Zn^{2+} with four water molecules and two imidazole ligands were also studied. The fully optimized structures of $[Zn(H_2O)_4(imidazole)_2]^{2+}$ and $\{[Zn(H_2O)_2(imidazole)_2]\cdot(H_2O)_2\}^{2+}$ are depicted in Figure 4. Note that in the octahedral complexes, the two heavy ligands prefer to be adjacent (rather than opposite) to one another. With two heavy ligands in the first coordination shell, the free energy gap between octahedral and tetrahedral zinc complexes in the gas phase widens even further: the ΔG_{isom}^{1} values are −8 and −14 kcal/mol for complexes containing one and two imidazoles, respectively (Table 3). Due to the more favorable gas-phase ΔG_{isom}^{1} for the cluster with two heavy ligands compared to the respective monosubstituted cluster, the 6 → (4 + 2) isomerization free energy remains negative in a buried ($\epsilon = 2$ or 4) as well as in solvent-exposed

Table 3. Enthalpies and Free Energies of Isomerization between Octahedral and Tetrahedral Complexes of Zn^{2+} and Mg^{2+} (in kcal/mol)

reaction	ΔH_{isom}^{1}	ΔG_{isom}^{1}	ΔG_{isom}^{2}	ΔG_{isom}^{4}	ΔG_{isom}^{80}
complexes with water					
$[Zn(H_2O)_6]^{2+} \leftrightarrow \{[Zn(H_2O)_4]\cdot(H_2O)_2\}^{2+}$	−2.3	−3.7	1.0	3.4	6.8
$[Mg(H_2O)_6]^{2+} \leftrightarrow \{[Mg(H_2O)_4]\cdot(H_2O)_2\}^{2+}$	5.3	4.3	9.6	12.3	15.5
complexes with one heavy ligand					
$[Zn(H_2O)_5(imidazole)]^{2+} \leftrightarrow \{[Zn(H_2O)_3(imidazole)]\cdot(H_2O)_2\}^{2+}$	−8.2	−8.4	−3.1	−0.4	2.7
$[Zn(H_2O)_5(HCOO)]^{+} \leftrightarrow \{[Zn(H_2O)_3(HCOO)]\cdot(H_2O)_2\}^{+}$	−5.4	−9.6	−8.1	−7.3	−6.3
$[Mg(H_2O)_5(imidazole)]^{2+} \leftrightarrow \{[Mg(H_2O)_3(imidazole)]\cdot(H_2O)_2\}^{2+}$	1.2	1.7	6.8	9.4	12.4
$[Mg(H_2O)_5(HCOO)]^{+} \leftrightarrow \{[Mg(H_2O)_3(HCOO)]\cdot(H_2O)_2\}^{+}$	7.2	3.1	4.9	5.9	7.0
complexes with two heavy ligands					
$[Zn(H_2O)_4(imidazole)_2]^{2+} \leftrightarrow \{[Zn(H_2O)_2(imidazole)_2]\cdot(H_2O)_2\}^{2+}$	−12.9	−13.9	−8.1	−5.3	−3.7

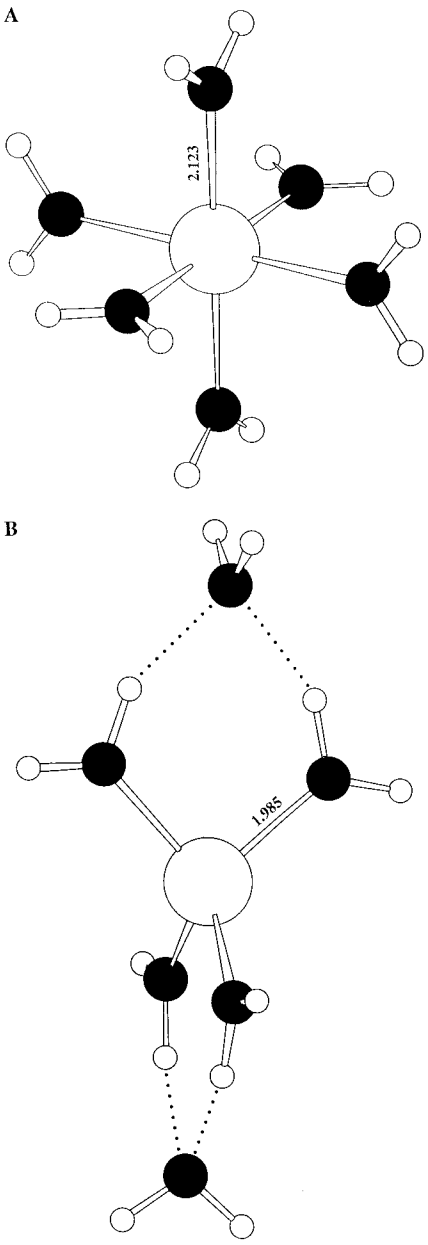

Figure 1. Ball-and-stick diagram of the fully optimized (A) octahedral Zn^{2+}−aqua complex and (B) (4 + 2) tetrahedral Zn^{2+}−aqua complex.

($\epsilon = 80$) zinc sites. The observed trends in the isomerization free energies indicate that as the number of neutral ligands coordinated to zinc increases, the free energy gap between the tetrahedral and octahedral complexes will widen, in favor of the tetrahedral species.

Binding Free Energies of Mg^{2+} and Zn^{2+} Complexes. To assess the factors that determine the metal cluster geometry, and, therefore, the difference between the coordination numbers found for Zn^{2+} and Mg^{2+} in the gas phase, the properties of zinc hydrates, $[Zn(H_2O)_n]^{2+}$ ($n = 1-6$), and zinc complexed with water and one imidazole, $[Zn(H_2O)_n(imidazole)]^{2+}$ ($n = 4-5$), were compared with those of the respective magnesium complexes. The calculated gas-phase binding free energies, ΔG_n^1, for $M^{2+} + nH_2O \rightarrow [M(H_2O)_n]^{2+}$, where M = Zn^{2+} or Mg^{2+} and $n = 1-6$, were computed using the B3LYP/6-31++G(2d,2p) optimized geometries and frequencies (see Methods). The difference between consecutive ΔG^1 values, i.e., $\Delta G_{n+1}{}^1 - \Delta G_n{}^1$, yielded the incremental binding free energies, $\Delta\Delta G_{n+1,n}{}^1$. The $\Delta G_n{}^1$, and $\Delta\Delta G_{n+1,n}{}^1$ values and the cation−ligand distances are summarized in Tables 4 and 5. The tables also list the partial atomic charges on the metal cation q_M as well as the change in q_M between consecutive reactions.

Table 4. Calculated Gas-Phase Binding Free Energies (ΔG^1), Incremental Binding Free Energies ($\Delta\Delta G^1$), Average M^{2+}−O Bond Distances ($\langle R_{M-O}\rangle$), and Partial Atomic Charges on the Metal (q_M) in $\{[M(H_2O)_n](H_2O)_m\}^{2+}$ Complexes (M = Mg, Zn)

reaction	ΔG^1 (kcal/mol)	$\Delta\Delta G^1$ (kcal/mol)	$\langle R_{M-O}\rangle$ (Å)	q_M[a] (electron)	$\Delta\Delta q_M$[b] (electron)
$Zn^{2+} + (n+m)H_2O \rightarrow \{[Zn(H_2O)_n](H_2O)_m\}^{2+}$					
$n = 1, m = 0$	−96.5	−96.5	1.87	1.89	0.11
$n = 2, m = 0$	−173.4	−76.9	1.86	1.76	0.13
$n = 3, m = 0$	−216.8	−43.4	1.94	1.74	0.02
$n = 4, m = 0$	−248.1	−31.3	2.00	1.73	0.01
$n = 5, m = 0$	−260.6	−12.5	2.07	1.71	0.02
$n = 4, m = 1$	−260.7		1.99	1.72	0.01
$n = 6, m = 0$	−270.0	−9.4	2.12	1.68	0.03
$n = 4, m = 2$	−273.7		1.99	1.72	0.00
$Mg^{2+} + (n+m)H_2O \rightarrow \{[Mg(H_2O)_n](H_2O)_m\}^{2+}$					
$n = 1, m = 0$	−73.0	−73.0	1.92	1.96	0.04
$n = 2, m = 0$	−134.0	−61.0	1.94	1.91	0.05
$n = 3, m = 0$	−178.2	−44.2	1.97	1.86	0.05
$n = 4, m = 0$	−211.4	−33.2	2.00	1.82	0.04
$n = 5, m = 0$	−226.9	−15.5	2.06	1.79	0.03
$n = 4, m = 1$	−223.7		2.00	1.82	0.00
$n = 6, m = 0$	−238.7	−11.8	2.10	1.75	0.04
$n = 4, m = 2$	−234.4		1.99	1.82	0.00

[a] Calculated according to NBO scheme. [b] Change in q_M between consecutive reactions.

Table 5. Calculated Gas-Phase Binding Free Energies (ΔG^1), Average M^{2+}−O and M^{2+}−N Bond Distances, and Partial Atomic Charges on the Metal (q_M) in $[M(H_2O)_n(imidazole)]^{2+}$ Complexes (M = Mg, Zn; $n = 4, 5$)

complex	ΔG^1 (kcal/mol)	$\langle R_{M-O}\rangle$ (Å)	$\langle R_{M-N}\rangle$ (Å)	q_M (electron)[a]
$Zn^{2+} + (n+m)H_2O$ + imidazole → $\{[Zn(H_2O)_n$imidazole$]\cdot(H_2O)_m\}^{2+}$				
$n = 4, m = 0$	−295.4	2.13	1.97	1.67
$n = 3, m = 1$	−298.5	2.03	1.94	1.67
$n = 5, m = 0$	−299.4	2.18	2.02	1.65
$n = 3, m = 2$	−307.8	2.02	1.95	1.67
$Mg^{2+} + (n+m)H_2O$ + imidazole → $\{[Mg(H_2O)_n$imidazole$]\cdot(H_2O)_m\}^{2+}$				
$n = 4, m = 0$	−254.1	2.08	2.07	1.76
$n = 3, m = 1$	−252.0	2.01	2.04	1.78
$n = 5, m = 0$	−262.6	2.13	2.13	1.73
$n = 3, m = 2$	−260.9	2.00	2.04	1.78

[a] Calculated according to NBO scheme.

(i) Complexes with Water. Table 4 shows that the binding of the first two water molecules to Zn^{2+} is more favorable than that to Mg^{2+}: the incremental free energies for Zn^{2+} are −97 and −77 kcal/mol, whereas the respective numbers for Mg^{2+} are −73 and −61 kcal/mol. However, addition of the third water molecule gives a similar incremental binding free energy (−43 kcal/mol for Zn^{2+} vs −44 kcal/mol for Mg^{2+}). After that, the incremental free energies for binding the fourth, fifth, and sixth water to Mg^{2+} become more negative (favorable) than the respective values for Zn^{2+} (Table 4). The observed change in the incremental binding free energy is reflected in the change in the metal−oxygen bond length. In the mono- and dihydrates, the Zn−O bond distance is shorter than the Mg−O bond length, but with each addition of a water molecule, it increases and becomes slightly longer than the Mg−O bond distance for the penta- and hexahydrated all-inner-shell complexes.

The trends in the incremental free energies of zinc and magnesium complexes can be rationalized in terms of the charge transfer from the ligand(s) to the metal cation. The initial

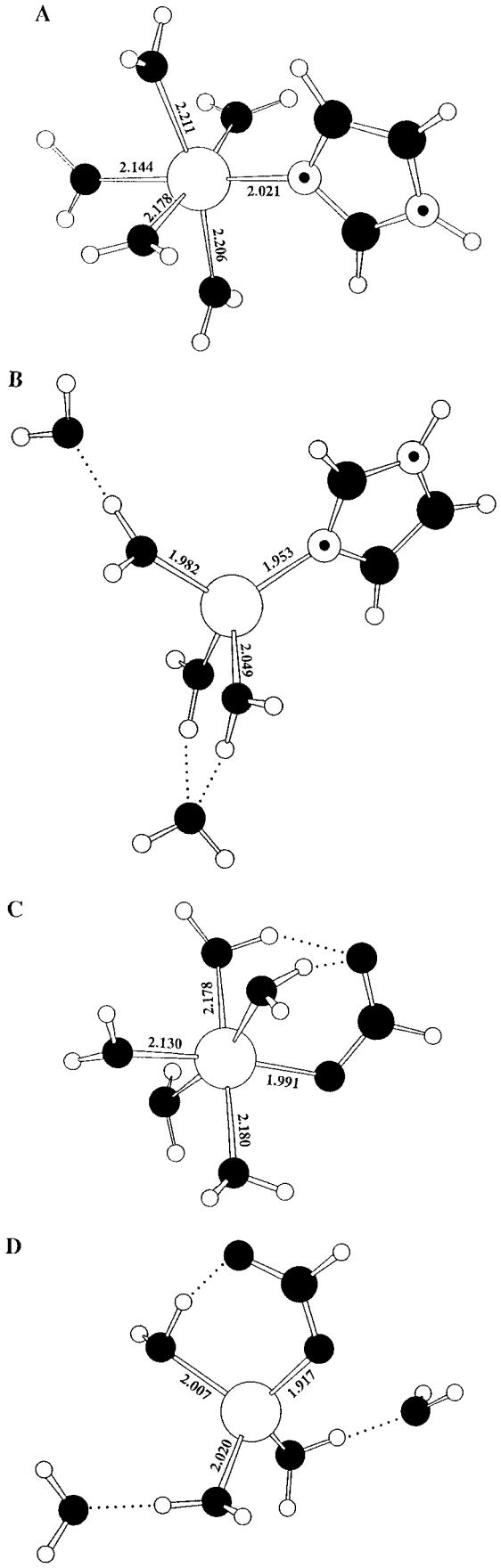

Figure 2. Ball-and-stick diagram of the fully optimized zinc complexes with water molecules and one heavy ligand: (A) octahedral complex with an imidazole; (B) tetrahedral complex with an imidazole; (C) octahedral complex with a formate; (D) tetrahedral complex with a formate.

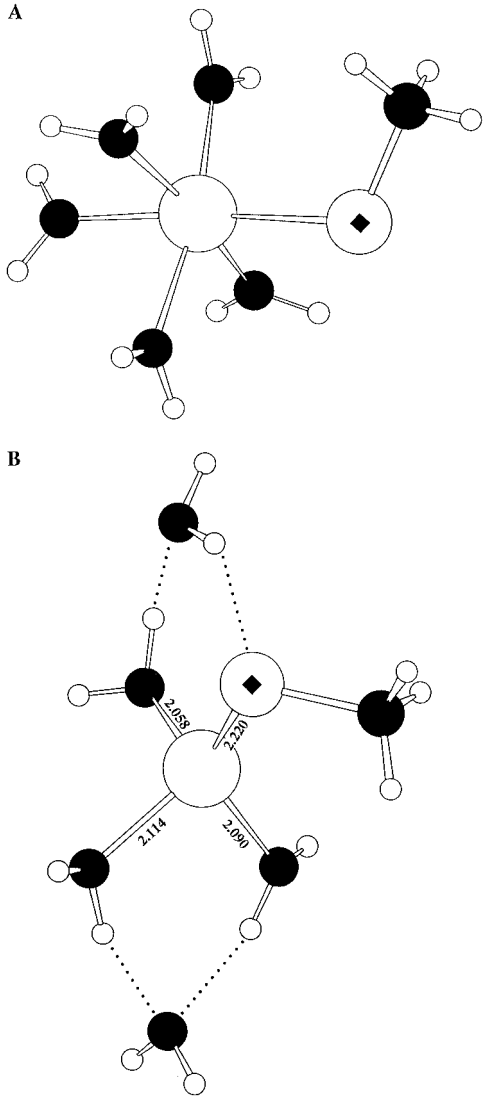

Figure 3. Ball-and-stick diagram of zinc complexes with water and a methanethiolate: (A) initial structure of the octahedral complex, which isomerized into a tetrahedral complex (with two waters in the outer sphere) during optimization; (B) fully optimized structure of the tetrahedral complex.

hydration process results in a greater transfer of electronic charge from water to zinc (0.11 e) than to magnesium (0.04 e), as evidenced by the lower positive charge on zinc (1.89 e) compared to that on magnesium (1.96 e). Similarly, the binding of the second water molecule results in an even greater transfer of electronic charge to zinc (0.13 e) compared to that to magnesium (0.05 e). However, the higher degree of neutralization of the positive charge on zinc upon binding the first two water molecules decreases the charge−dipole and charge−induced dipole interactions (which depend on the magnitude of the charge on the metal). Hence, the magnitude of $\Delta\Delta G^1$ of subsequent water binding to zinc decreases and becomes less than the respective values for magnesium.

The charge transfer from the ligand(s) to the metal cation seems to regulate not only the incremental binding free energies but also the geometry of the cluster. Whether a water molecule will be placed in the inner or outer coordination shell of the metal depends on the relative free energy gain for these two positions. Comparison of the pentaaqua isomers shows that the absolute binding free energies for the pentacoordinated $[Zn(H_2O)_5]^{2+}$ (−260.6 kcal/mol) and tetracoordinated $\{[Zn(H_2O)_4]\cdot(H_2O)_1\}^{2+}$ (−260.7 kcal/mol) complexes are almost equal,

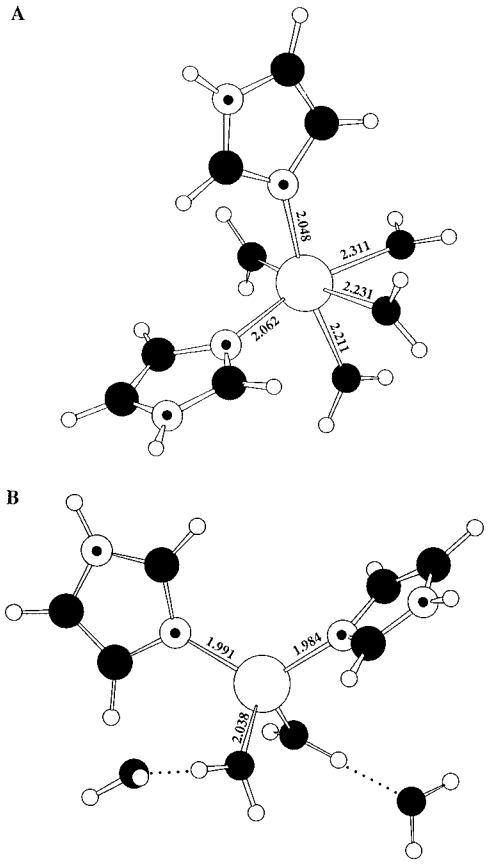

Figure 4. Ball-and-stick diagram of the fully optimized zinc complexes with water and two imidazoles: (A) octahedral complex; (B) tetrahedral complex.

whereas $[Mg(H_2O)_5]^{2+}$ is more stable (by −3.2 kcal/mol) than $\{[Mg(H_2O)_4]\cdot(H_2O)_1\}^{2+}$. For the hexaaqua isomers, the tetrahedral $\{[Zn(H_2O)_4]\cdot(H_2O)_2\}^{2+}$ structure is more stable (by −3.7 kcal/mol) than the respective octahedral $[Zn(H_2O)_6]^{2+}$ complex; in contrast, octahedral $[Mg(H_2O)_6]^{2+}$ is more stable (by −4.3 kcal/mol) than tetrahedral $\{[Mg(H_2O)_4]\cdot(H_2O)_2\}^{2+}$. These observations may be rationalized in terms of the large charge transfer from the first two water molecules to zinc, which results in a lower net positive charge on zinc compared to that on magnesium for complexes of a given coordination number. The relatively low positive charge on zinc in the hexaaqua complexes probably disfavors binding of a water molecule in the inner sphere compared to that in the outer sphere; conversely, the greater positive charge on magnesium in the penta- and hexahydrates favors the inner-sphere binding mode.

(ii) Complexes Containing Water and Heavy Ligands. The general trends in the changes in incremental free energies and the partial charges on the metal for zinc and magnesium mixed-ligand complexes are similar to those found for the respective all-water complexes. (a) The charge on zinc is lower than that on magnesium for complexes of a given coordination number. (b) Tetrahedral (4 + 1) and (4 + 2) zinc complexes are more stable than the respective all-inner-sphere complexes. (c) Magnesium prefers an all-inner-sphere ligand surrounding when the coordination number is ≤6. Note, however, that the positive charge on zinc or magnesium in the imidazole-containing complex is lower than that in the respective all-water complex due to the stronger charge transfer from imidazole compared to that from water.[33]

The free energy difference between the Zn^{2+}−water−imidazole isomers is larger than that between the respective Zn^{2+}−water clusters. For the mixed-ligand structures, $\Delta G_{4+1} - \Delta G_5 = -3.1$ kcal/mol and $\Delta G_{4+2} - \Delta G_6 = -8.4$ kcal/mol; for the all-water structures, the respective numbers are −0.1 and −3.7 kcal/mol. The greater stability of the tetrahedral species in the Zn^{2+}−water−imidazole series appears to be related to the further decrease of the positive charge on zinc, which probably makes binding of a water molecule in the inner sphere even less favorable than that in the case of the metal hydrates. Similarly, the greater neutralization of the positive charge on zinc by negatively charged ligands such as formate and methylthiolate compared to that by imidazole and water contributes, in part, to the stability of the tetrahedral structure relative to its octahedral counterpart.

(33) Garmer, D. R.; Gresh, N. *J. Am. Chem. Soc.* **1994**, *116*, 3556.

Discussion

Assessment of Errors. In computing the isomerization free energies in Table 3, systematic errors in the computed gas-phase and solvation free energies of the reactants are likely to partially cancel those of the respective products. Errors in the computed gas-phase energies have been minimized by calibrating the basis set employed (see Results and Table 1). Errors in the computed gas-phase entropies stem from two sources: (a) inaccuracies in the low-frequency skeletal modes and (b) inaccurate treatment of these modes. The former can be attributed mainly to the neglect of anharmonicity in computing the frequencies. However, it has been shown that anharmonicity effects do not contribute significantly to the vibrational entropy.[34,35] Errors in the entropies stemming from (b) were assessed by excluding the lowest frequency modes (below 20 cm^{-1}) from the entropy evaluation. The resulting $T\Delta S_{isom}$ values deviate from the respective entropies evaluated by employing the full set of frequencies by 0.5−2.1 kcal/mol, but the general trends in the isomerization free energies observed in Table 3 remain the same (see Results).

On the other hand, the computed $\Delta G_{solv}{}^{x}$ are subject to errors stemming from (a) the assumption of the gas-phase geometry in the different dielectric environments, (b) uncertainties in the dielectric boundary, and (c) the neglect of nonelectrostatic forces. These three sources of error have been taken into account implicitly in computing $\Delta G_{solv}{}^{80}$ by using a set of atomic radii that have been adjusted to reproduce the experimental hydration free energies of the metal dications and ligands, as well as the solution free energies of water → chloride substitution reactions (Table 2). Furthermore, errors in $\Delta G_{solv}{}^{x}$ stemming from (a) are probably not serious, judging from the small change in the metal−oxygen(water) distance in different dielectric environments. The mean Zn−O(water) distance from *octahedral* structures in the Cambridge Structural Database (CSD) and aqueous solution is 2.11 ± 0.07[7] and 2.10 ± 0.07[6] Å, respectively, which is close to the computed Zn−O distance of 2.12 Å for $[Zn(H_2O)_6]^{2+}$ (see Table 4). Errors in $\Delta G_{solv}{}^{x}$ due to (b) have been reduced by including the first coordination shell around the metal explicitly, thus extending the dielectric boundary from the central metal atom.

Comparison with Experiment and Previous Theoretical Studies. (i) Gas Phase. The computed geometries and coordination numbers for the gas-phase metal complexes are in accord with available experimental data and/or previous theoretical studies. The average Zn−O(water) distances in Tables 4 and 5

(34) Loewenschuss, A.; Marcus, Y. *Chem. Rev.* **1984**, *84*, 89.

(35) Chase, M. W.; Davies, C. A.; Downey, J. R.; Fruip, D. J.; McDonald, R. A.; Syverud, A. N. *J. Phys. Chem. Ref. Data, Suppl.* **1985**, *14*, 1.

are in quantitative agreement with those observed in hydrated zinc crystal structures in the CSD. The average Zn−O(water) distances for four-, five-, and six-coordinate zinc (from Tables 4 and 5) are 1.99−2.03, 2.07−2.13, and 2.12−2.18 Å, respectively, whereas the corresponding CSD distances are 2.01 ± 0.03, 2.05 ± 0.07, and 2.11 ± 0.07 Å.[7] The finding that the (4 + 2) tetrahydrated zinc complex is the stablest structure in the gas phase and the trends in the metal−O bond distances and hydration free energies of zinc and magnesium complexes are in line with calculations by Pavlov et al.[15] (see Introduction). In contrast to zinc hydrates, octahedral magnesium complexes are predicted to be the dominant species in the gas phase, in agreement with experimental observations.[36]

(ii) Condensed Media. The results in Table 3 predict both Mg^{2+} and Zn^{2+} to be octahedrally coordinated in aqueous solutions, in accord with X-ray diffraction studies reporting a coordination number of 6 for Mg^{2+} and Zn^{2+} in aqueous salt solutions.[6] The predicted coordination number for the zinc complexes containing at least one heavy ligand in a protein environment is also in accord with that observed in the Protein Data Bank (PDB) structures with the same coordinating ligand types. The trends in the results in Table 3 indicate that zinc bound to water molecules and two or more imidazoles is likely to be tetrahedrally coordinated. All PDB structures containing zinc bound to water molecules and two or more imidazoles indeed show zinc to be tetrahedrally coordinated (Lin and Lim, unpublished results).[7]

Factors Governing the Coordination Number of Zinc. The results in Table 3 predict that in the *gas* phase, zinc prefers to be tetrahedrally hydrated, due, in part, to the large charge transfer from the first two water molecules to zinc (Table 4). In *aqueous* solution, however, zinc prefers to be octahedrally coordinated because the octahedral complex is better hydrated than the tetrahedral (4 + 2) structure. In a *protein* environment, zinc can adopt either an octahedral or a tetrahedral geometry, depending on the type of protein ligand it is bound to and the solvent accessibility of the metal-binding site. For zinc bound to water molecules and one *neutral* ligand, like the deprotonated histidine side chain, zinc prefers to be tetrahedrally coordinated if the binding site is buried ($\epsilon < 4$), but it may adopt an octahedral geometry if the zinc site is characterized by $\epsilon > 4$. For zinc bound to water molecules and two or more neutral histidine side chains, the free energy difference between the isomeric tetrahedral and octahedral clusters increases so that the tetrahedral structure is dominant in both buried and solvent-exposed binding sites**.** Similarly, for zinc bound to water molecules and one *negatively charged* ligand, like the ionized side chain of cysteine, aspartic acid, or glutamic acid, tetrahedral coordination is predicted, regardless of the solvent accessibility of the zinc site.

Strain Hypothesis. The catalytic activity of zinc-containing enzymes has been explained in terms of energized (entatic) states of the metal binding site(s).[9] In this hypothesis, six-coordinate *octahedral* Zn^{2+}, as found in aqueous solutions, is assumed to be the ground-state geometry, while deviation from the coordination number of 6 to 5 or 4 are assumed to yield strained structures. It is also assumed that the protein structure is a rigid frame, whose steric demands forces the zinc cation to adopt four- or five-coordinate geometry upon binding to the protein, thus creating strained energized states. In other words, the protein fails to provide the expected arrangement of ligating groups, which is assumed to be octahedral, thereby forcing the metal into an unusual, energized geometric state.[9]

Our calculations show that, in complexes with one acidic or two or more neutral ligands (characteristic of catalytic binding sites), zinc prefers to be *tetracoordinated* in both the gas phase and protein cavities. Thus, it appears that *tetrahedral* zinc-binding sites are not necessarily energized states, and the contribution of "coordination strain" to the catalytic activity of zinc enzymes may not be significant. Instead, five- and six-coordinate structures are expected to represent energized states in proteins; i.e., they may be less stable than the four-coordinate counterpart. It should be noted that a tetracoordinated zinc site may possess some degree of strain due to the protein-matrix-induced deviations from an ideal tetrahedral geometry, but this is expected to be smaller than the strain caused by changing the coordination number from 4 to 5 or 6. These findings agree with the results obtained by Ryde, who, in modeling the alcohol dehydrogenase active site, showed that *tetracoordinated* zinc structures are more stable (i.e., less strained) than the respective *pentacoordinated* species by 24−48 kcal/mol.[18]

Our finding that the *tetrahedral* zinc complexes in protein cavities generally represent the optimal, least strained structures among various zinc polyhedra may explain why four-coordinate zinc is chosen to play a structural role in zinc fingers and enzymes (see Introduction). Furthermore, the four-coordinate structures have shorter metal−ligand distances than the respective five- or six-coordinate all-inner-sphere structures (Tables 4 and 5). The low strain in combination with shorter metal−ligand bond lengths secures tighter binding, making tetrahedral zinc-binding sites well suited for stabilizing a given protein fold or configuration. Our finding is in accord with the fact that nearly all *structural* zinc binding sites (excluding multimetal sites) found to date are tetrahedrally coordinated[7,37] (Lin and Lim, unpublished results).

Conclusions

(1) The lowest-energy ground-state coordination number of zinc bound to one acidic or two or more neutral protein ligands is likely to be 4. Hence, it appears unlikely that tetrahedral zinc-binding sites represent energized ground states in zinc-containing enzymes. The lack of strain seems to contribute to the stability of *structural* tetracoordinated zinc sites.

(2) Hydrated zinc with a coordination number of 6 undergoes a change in the coordination geometry upon binding to the first or second amino acid residue. The observed decrease in the coordination number of zinc upon protein binding reflects primarily the requirements of the metal and ligands, rather than the constraints of the protein matrix on the metal. It is partly due to the greater charge transfer to zinc from heavy ligand(s) compared to that from water, as well as to the greater charge transfer from a given ligand type to zinc compared to that to magnesium upon ligand binding.

Acknowledgment. We are grateful to D. Bashford, M. Sommer, and M. Karplus for the program to solve the Poisson equation. T.D. is supported by a fellowship from the Institute of Biomedical Sciences. This work is supported by the Institute of Biomedical Sciences at Academia Sinica, the National Center for High Performance Computing, and the National Science Council, Republic of China (NSC-88-2113-M-001).

JA0010296

(36) Peschke, M.; Blades, A. T.; Kebarle, P. *J. Phys. Chem. A* **1998**, *102*, 9978.

(37) Coleman, J. E. *Annu. Rev. Biochem.* **1992**, *61*, 897.